FINITE ELEMENTS IN FLUIDS

Homework 2
Viscous Incompressible Flows

Submitted by
Karthik Neerala Suresh
M.Sc. Computational Mechanics
Universitat Politècnica de Catalunya, BarcelonaTECH

Submitted to
Dr. Esther Sala
Lecturer
Universitat Politècnica de Catalunya, BarcelonaTECH

22 May 2017

Contents

List of Figures

1. Cavity Flow Problem

The cavity flow problem is a standard benchmark test for incompressible flows. The goal of this exercise is to analyse the results obtained when adopting either the Stokes or the Navier-Stokes equations. Using the code in (`HW2Files_Cavity`) to compute the finite elements approximation of these problems the tasks given in the Homework are completed.

(1) Using the script `mainStokes.m` the solution of the Stokes problem is computed using a uniform, structured mesh of Q_2Q_0, Q_2Q_1, P_1P_1 and MINI ($P_1^+P_1$) elements, with 20 elements per side. Fig. 1.1, 1.2, 1.3 and 1.4 show the various plots obtained for these cases.

The Q_2Q_0 is a quadrilateral element in which the velocity is approximated using biquadratic interpolation polynomials, while the pressure is approximated to a constant within each element (see Fig. 1.1a and 1.1c). This element satisfies the LBB condition. It can be seen from Fig. 1.1b and 1.1d that both velocity and pressure profiles are devoid of any spurious non physical oscillations. Since pressure is approximated using constants per element, pressure is discontinuous between elements.

The Q_2Q_1 is a quadrilateral element in which the velocity is approximated using biquadratic interpolation polynomials, while the pressure is approximated to a bilinear interpolation polynomials within each element (see Fig. 1.2a and 1.2c). This element satisfies the LBB condition. It can be seen from Fig. 1.2b and 1.2d that both velocity and pressure profiles are devoid of any spurious non physical oscillations. Unlike with the case with Q_2Q_0 element, the pressure is a continuous as it is approximated using bilinear polynomials.

The P_1P_1 is a triangular element in which the velocity and pressure are both approximated using linear interpolation polynomials (see Fig. 1.3a and 1.3c). This element does not satisfy the LBB condition. It can be seen from Fig. 1.3b and 1.3d that while the streamlines of velocity look to be without much disturbance, the pressure field is full of spurious non physical oscillations. This kind of element needs stabilisation to obtain pressure fields that are physical. Also though the streamlines of velocity seem to be correct, there are some non physical oscillations near the walls.

Finally The MINI ($P_1^+P_1$) is a triangular element in which the velocity and pressure

are both approximated using linear interpolation polynomials (see Fig. 1.4a and 1.4c). However the velocity interpolation is complemented with a cubic bubble function which ensures that this element satisfies the LBB condition. It can be seen from Fig. 1.4b and 1.4d that while the streamlines of velocity and the pressure field are devoid of any spurious non physical oscillations.

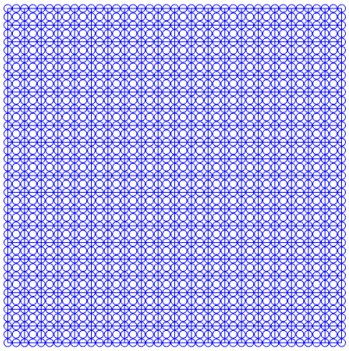

(a) Mesh for velocity

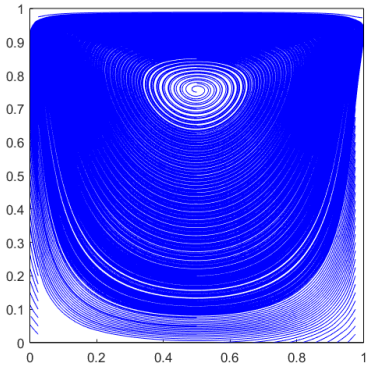

(b) Streamlines

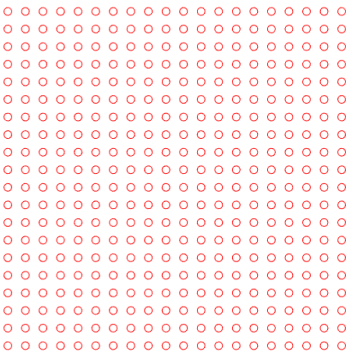

(c) Mesh for pressure

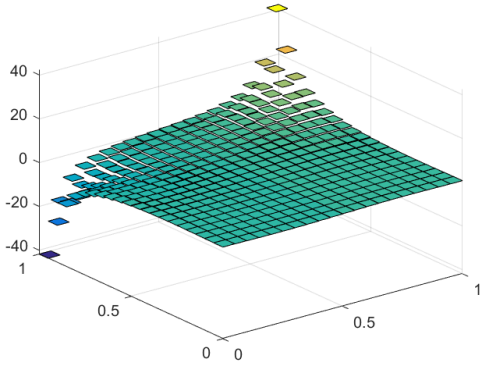

(d) Pressure

Figure 1.1: Results with Q_2Q_0 elements

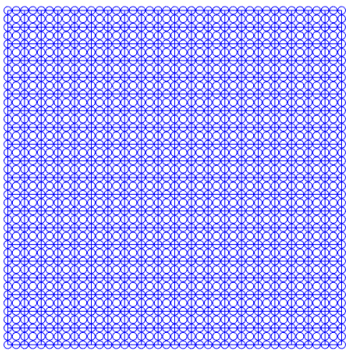

(a) Mesh for velocity

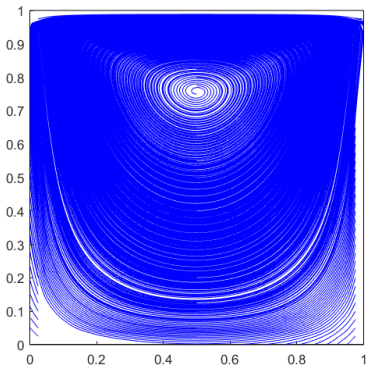

(b) Streamlines

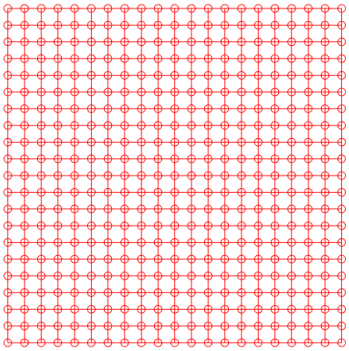

(c) Mesh for pressure

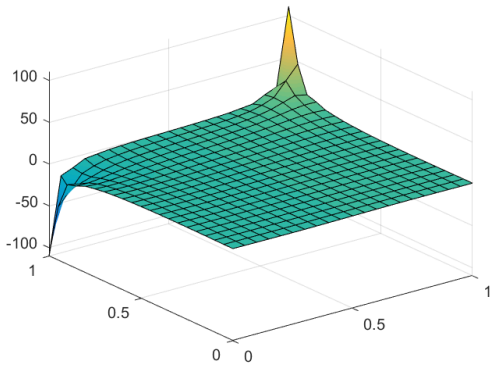

(d) Pressure

Figure 1.2: Results with Q_2Q_1 elements

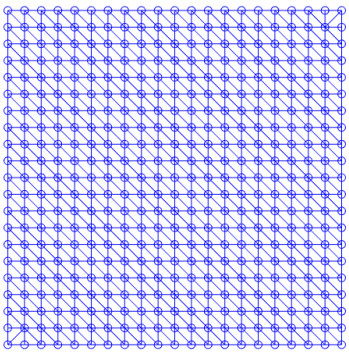

(a) Mesh for velocity

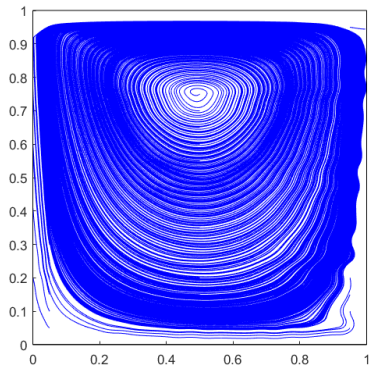

(b) Streamlines

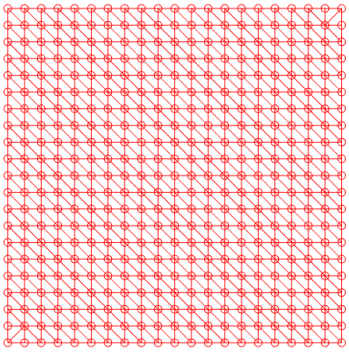

(c) Mesh for pressure

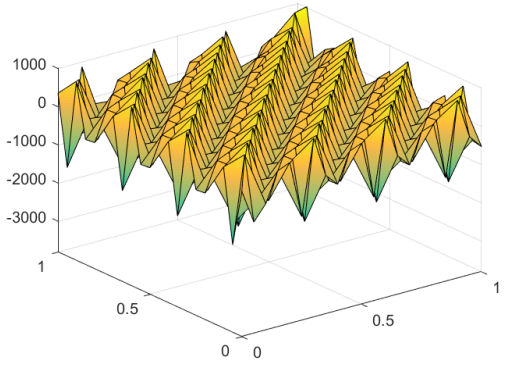

(d) Pressure

Figure 1.3: Results with P_1P_1 elements

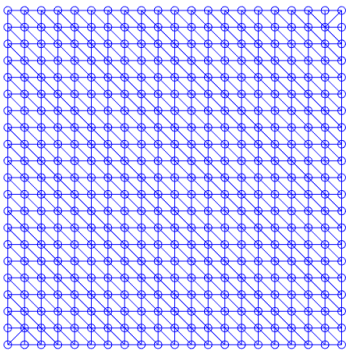

(a) Mesh for velocity

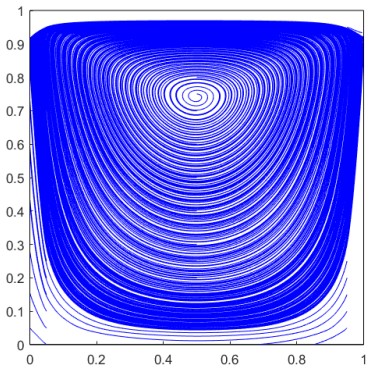

(b) Streamlines

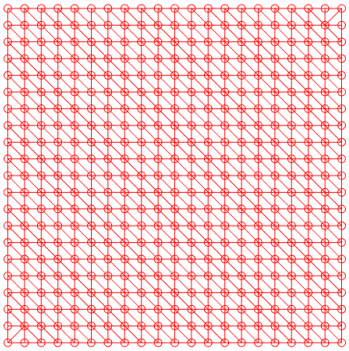

(c) Mesh for pressure

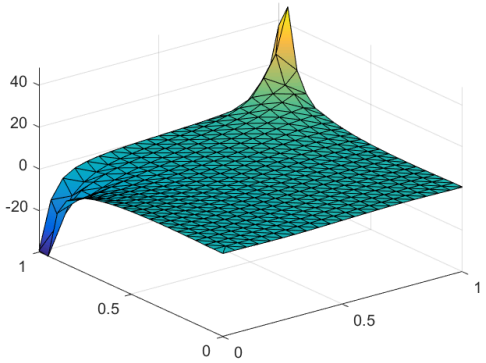

(d) Pressure

Figure 1.4: Results with MINI $P_1^+P_1$ elements

(2) The solution of the Stokes problem considering (i) a structured, uniform mesh of Q_2Q_1 elements with 20 elements per side (ii) a structured mesh of 20×20 Q_2Q_1 elements refined near the walls are computed and compared.

Fig. 1.2a and 1.2c show the mesh used for approximating velocity and pressure while using a structured, uniform mesh, while Fig. 1.5a and 1.5c show the mesh used for approximating velocity and pressure while using an adaptive mesh refined near the boundaries. The streamlines and pressure field for the case with the uniform structured mesh are shown in Fig. 1.2b and 1.2d, while Fig. 1.5b and 1.5d show these for the adapted mesh. While the streamlines appear to be more or less similar, there is a stark contrast in the plots of the pressure fields. While using the mesh with adaptive refinement around the boundaries, the discontinuities in pressure at the boundaries are captured much more clearly. The pressure field in this case has a much more sharper discontinuity at the boundaries than the case when elements of uniform size are used throughout the mesh. This can also be seen from the magnitude of the pressure at the boundaries (in the case of the adaptive

mesh it is of the order of ± 1000, while it is of the order of ± 100 in the case of the uniform mesh). Since both the meshes have same number of elements, and hence degrees of freedom, their computational costs are the same. Hence, it is definitely better to use a mesh with adaptive refinement around the boundaries to solve the calvity problem as the solution obtained in this case for the pressure field is more accurate.

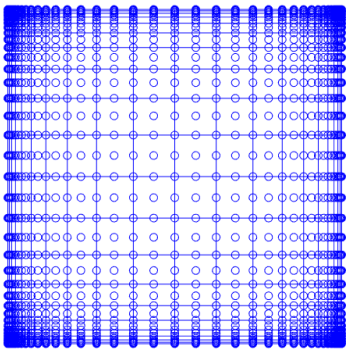

(a) Mesh for velocity

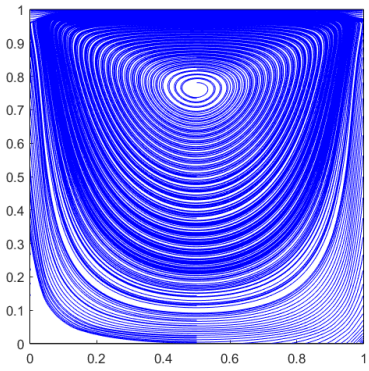

(b) Streamlines

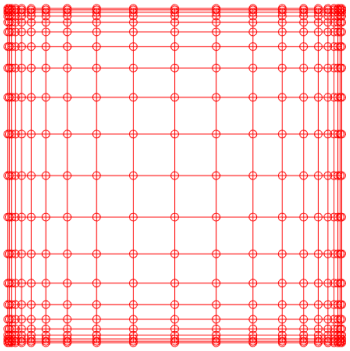

(c) Mesh for pressure

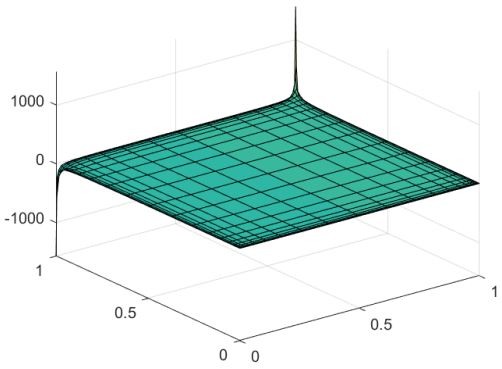

(d) Pressure

Figure 1.5: Results with Q_2Q_1 elements refined near the walls

(3) The Stokes code is modified to solve the problem using a GLS stabilized formulation with P_1P_1 elements. The stabilization of the Stokes problem is obtained by adding to the Galerkin weak form of the Stokes equations, the equations emanating from the least-squares form, which are

$$\begin{cases} (-\nu\boldsymbol{\nabla}^2\boldsymbol{w}, -\nu\boldsymbol{\nabla}^2\boldsymbol{v} + \boldsymbol{\nabla}p - \boldsymbol{b}) = 0 & \forall \boldsymbol{w} \in \boldsymbol{\mathcal{V}} \\ (\boldsymbol{\nabla}q, -\nu\boldsymbol{\nabla}^2\boldsymbol{v} + \boldsymbol{\nabla}p - \boldsymbol{b}) = 0 & \forall q \in \mathcal{Q} \end{cases}$$

To avoid additional continuity requirements due to the presence of second spatial derivatives, the terms added to the Galerkin weak form act on the element interiors

only. These terms depend on the residual of the momentum equation and therefore ensure the consistency of the stabilized formulation.

For linear elements the GLS stabilization does not affect the weak form of the momentum equation because the terms involving the second derivatives of the weighting function w vanish. The GLS weak formulation then reduces to the following variational problem: find $\boldsymbol{v}^h \in \boldsymbol{\mathcal{S}}^h$ and $p^h \in \mathcal{Q}^h$, such that, for all $(\boldsymbol{w}^h, q^h) \in \boldsymbol{\mathcal{V}}^h \times \mathcal{Q}^h$

$$\begin{cases} \boldsymbol{a}(\boldsymbol{w}^h, \boldsymbol{v}^h) + \boldsymbol{b}(\boldsymbol{w}^h, p^h) = (\boldsymbol{w}^h, \boldsymbol{b}^h) + (\boldsymbol{w}^h, \boldsymbol{t}^h)_{\Gamma_N}, \\ \boldsymbol{b}(\boldsymbol{v}^h, q^h) - \sum_{e=1}^{\mathtt{nel}} \tau_e (\boldsymbol{\nabla} q^h, \boldsymbol{\nabla} p^h)_{\Omega^e} = -\sum_{e=1}^{\mathtt{nel}} \tau_e (\boldsymbol{\nabla} q^h, \boldsymbol{b}^h)_{\Omega^e} \end{cases}$$

Note that the second term in the second equation indicates that a Poisson equation has been generated for the pressure field. A consequence of the GLS stabilization of the Stokes problem is that elements with equal order interpolations, which are unstable in the Galerkin formulation, now become stable.

The stabilization parameter chosen in the code is

$$\tau_e = \alpha \frac{h_e^2}{4\nu}$$

In the tests, different values of α are chosen to see the effect of GLS stabilisation on the solution. Fig. 1.6 and 1.7 show the plots of streamlines and pressure field obtained for values of $\alpha = 2, 20, 200, 2000$. From the figures it can be clearly seen that as the value of the stabilization parameter is increased, there is a degradation in the streamlines. It appears that the streamlines start to get convected upon increasing the stabilization. However, pressure field shows that increasing the stabilization makes it more and more accurate. For $\alpha = 2$, the pressure field has non physical oscillations, while for $\alpha = 200$ and 2000, the streamlines are not physical solutions to the cavity problem. Thus it is important to choose a value of α in τ which gives enough stabilization to pressure while retaining the true value of velocity.

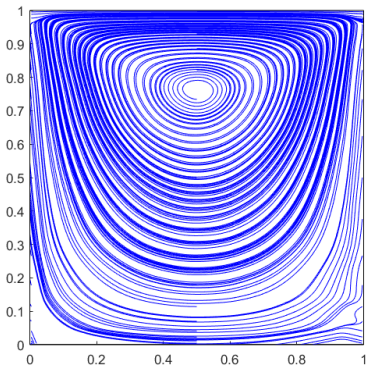

(a) $\alpha = 2$

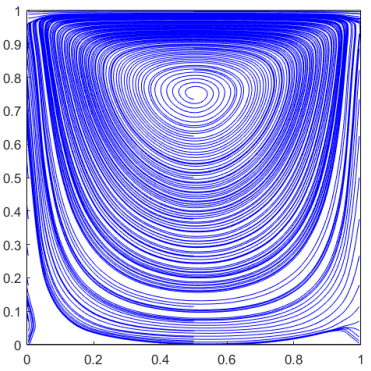

(b) $\alpha = 20$

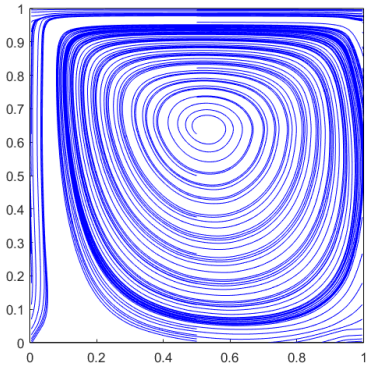

(c) $\alpha = 200$

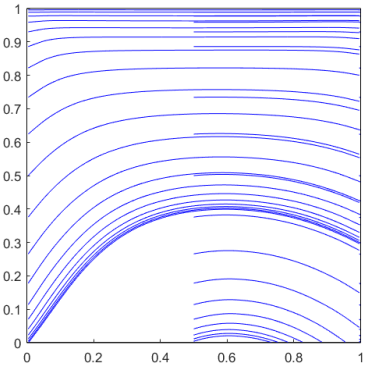

(d) $\alpha = 2000$

Figure 1.6: Streamlines obtained by solving cavity problem using GLS stabilized formulation with P_1P_1 elements with different values of α in stabilization parameter

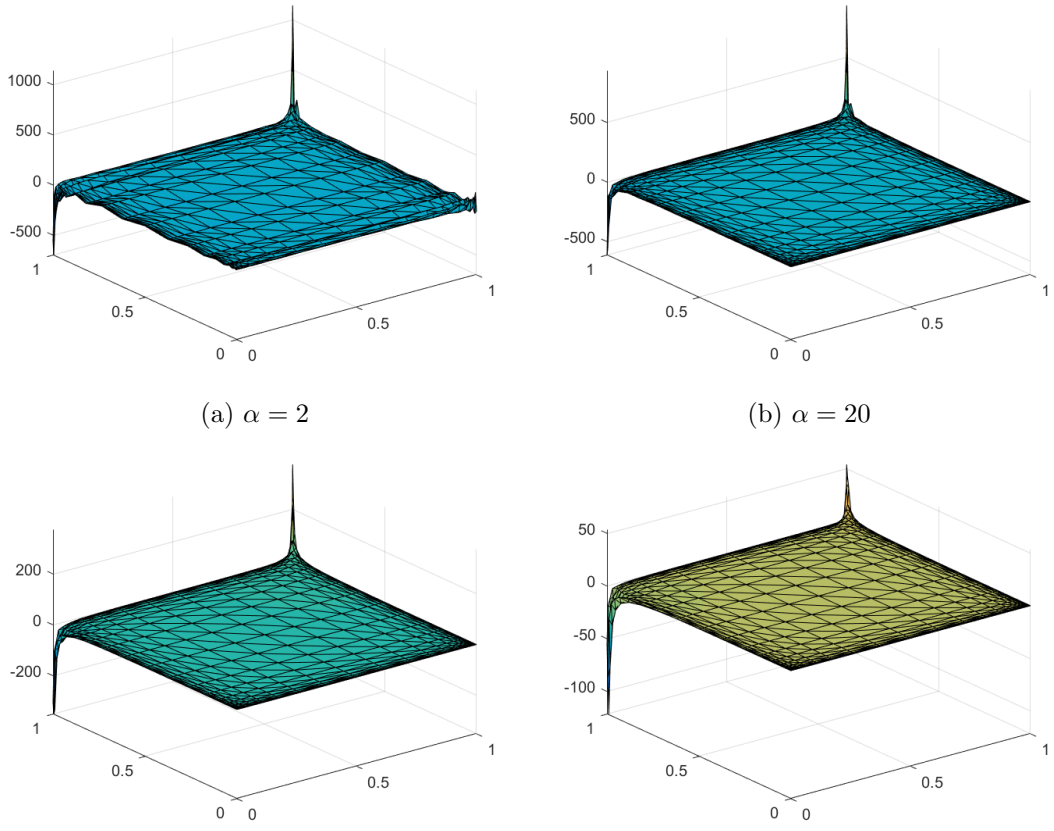

(a) $\alpha = 2$ (b) $\alpha = 20$

(c) $\alpha = 200$ (d) $\alpha = 2000$

Figure 1.7: Pressure field obtained by solving cavity problem using GLS stabilized formulation with P_1P_1 elements with different values of α in stabilization parameter

(4) The script `mainNavierStokes.m` is used to solve the Navier-Stokes equations with Picard method after writing a Matlab function `ConvectionMatrix.m` to evaluate the matrix arising from the discretization of the convective term. The Navier-Stokes equations is solved using a structured mesh of Q_2Q_1 elements with 20 elements per side, considering the Reynolds numbers $Re = 100, 500, 1000, 2000$. The results obtained from the run of the code are shown in Fig. 1.9 and 1.10. The number of iterations required for convergence of Picard method are tabulated in Table 1.1

Table 1.1: Number of iterations required for convergence of Picard method

Re	Number of Iterations
100	13
500	29
1000	35
2000	69

From Table 1.1 it can be seen that upon increasing Re, the number of iterations required for the convergence of Picard Method go on increasing. From Fig. 1.9 it can be seen that as Re is increased the position of the main vortex moves towards the center of the cavity. Also the strength of the main vortex goes on decreasing with increase in Re. The development of a secondary vortex in the right bottom corner of the cavity becomes progressively apparent and a third vortex appears at the lower left corner as seen in 1.9a, 1.9b and 1.9c. Elevated velocity gradients develop near the cavity walls for large values of the flow Re. This generates non-physical oscillations in the Galerkin solution for the velocity (see Fig. 1.9d). A stabilized formulation would then be required.

These results are in excellent agreement with the results obtained from literature (see Donea and Huerta, Finite Element Methods for Fluid Flow Problems, Wiley 2003). Fig 1.8 for the solution given in the reference.

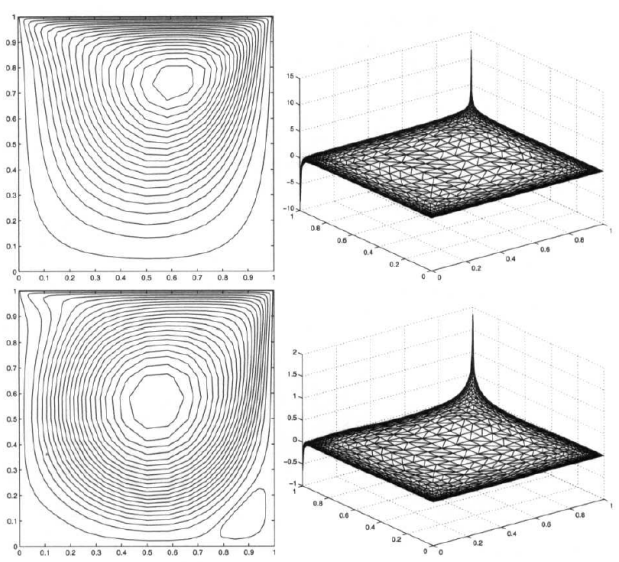

Fig. 6.12 Cavity: `Mini` element, streamlines and pressure for $Re = 100$ (top) and 1000 (bottom).

Figure 1.8: Reference Solution

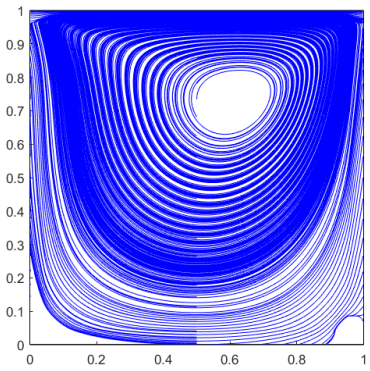

(a) $Re = 100$

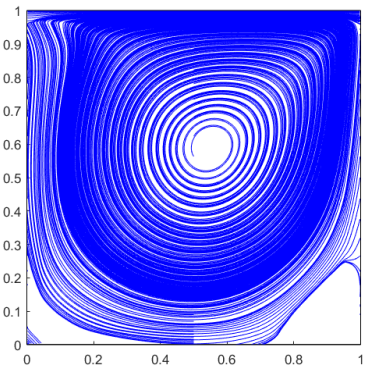

(b) $Re = 500$

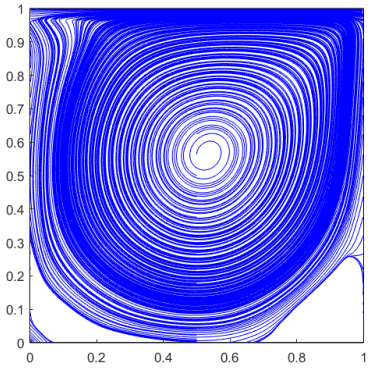

(c) $Re = 1000$

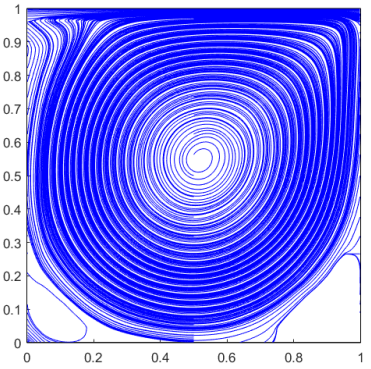

(d) $Re = 2000$

Figure 1.9: Streamlines obtained by solving cavity problem using Navier-Stokes equations with Picard method with Q_2Q_1 elements with different values of Reynold's number, Re

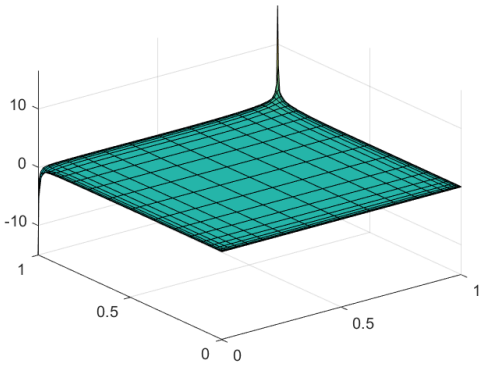

(a) $Re = 100$

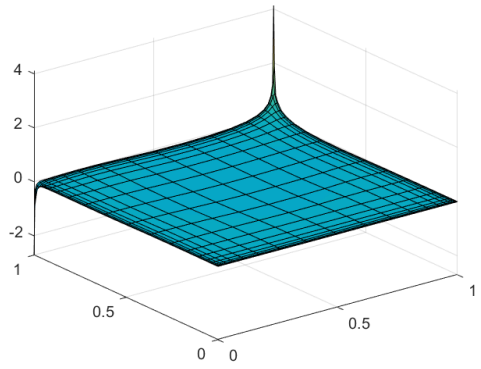

(b) $Re = 500$

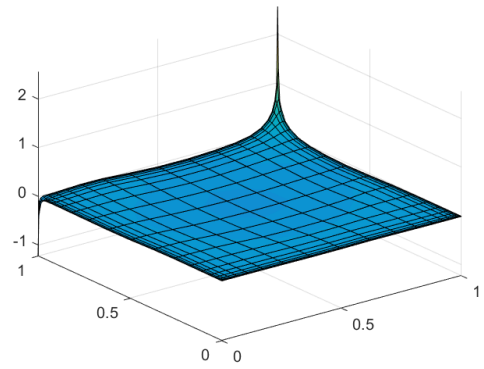

(c) $Re = 1000$

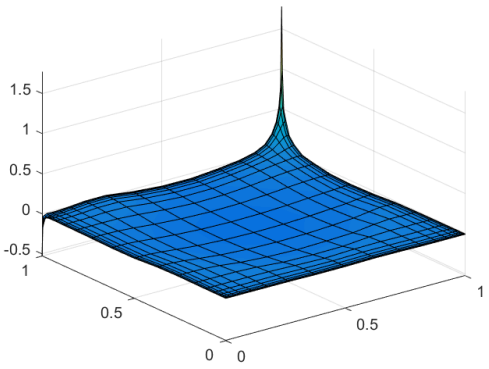

(d) $Re = 2000$

Figure 1.10: Pressure field obtained by solving cavity problem using Navier-Stokes equations with Picard method with Q_2Q_1 elements with different values of Reynold's number, Re